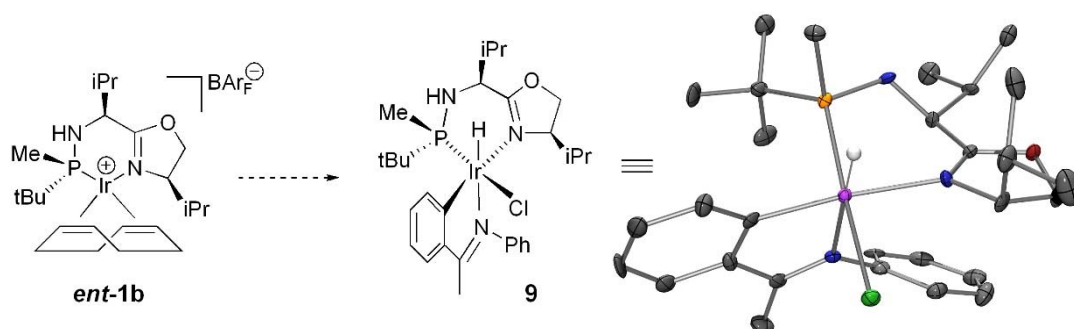


P-Stereogenic and Non P-Stereogenic Ir-MaxPHOX in the Asymmetric Hydrogenation of *N*-Aryl Imines. Isolation and X-ray Analysis of Imine-Iridacycles.

Ernest Salomó,[†] Pep Rojo,[†] Pol Hernández-Lladó,[†] Antoni Riera,^{†,‡,*} Xavier Verdaguer^{†,‡,*}

[†] Institute for Research in Biomedicine (IRB Barcelona), Barcelona Institute of Science and Technology, Baldori Reixac 10, 08028 Barcelona, Spain.

[‡] Dept. Química Inorgànica i Orgànica, Secció de Química Orgànica, Universitat de Barcelona, Martí i Franquès 1, 08028 Barcelona, Spain.



ABSTRACT: A small library of Ir-MaxPHOX catalysts has been applied to the asymmetric hydrogenation of *N*-aryl imines. A structure-activity analysis of the three

chiral center MaxPHOX ligand has been performed. Using complex **1b**, the hydrogenation of *N*-aryl imines took place with up to 96% enantiomeric excess at atmospheric pressure of hydrogen and low temperature. The impact of the stereochemical information at the phosphorous center is small with respect the selectivity, but large with respect the catalyst activity. Non P-stereogenic analogs of MaxPHOX were also synthesized and tested but provided lower selectivity. The selectivity observed could be explained by taking into account that the actual catalysts were cyclometalated imine complexes formed *in situ*. [IrHCl(MaxPHOX)(imine)] complexes **9** and **10** were synthesized and characterized by X-ray crystallography. These complexes, *via* chloride abstraction, provided the active catalytic species with the same levels of selectivity. Finally, the influence of the counter ion on the catalyst performance was also studied.

INTRODUCTION

Many active pharmaceutical ingredients and agrochemicals contain chiral amines. In this regard, there is considerable interest in developing efficient methods that provide single enantiomers of such compounds, thus avoiding inefficient racemate resolutions. Metal-catalyzed asymmetric hydrogenation of imines is one of the methods of choice in terms of industrial applicability.¹ While ruthenium has provided excellent results in transfer-hydrogenation reactions, iridium has shown better performance for the direct hydrogenation of imines.² In this field, Pfaltz and others have shown that Ir-P,N catalysts provide an excellent platform for the reduction of *N*-aryl imines.³

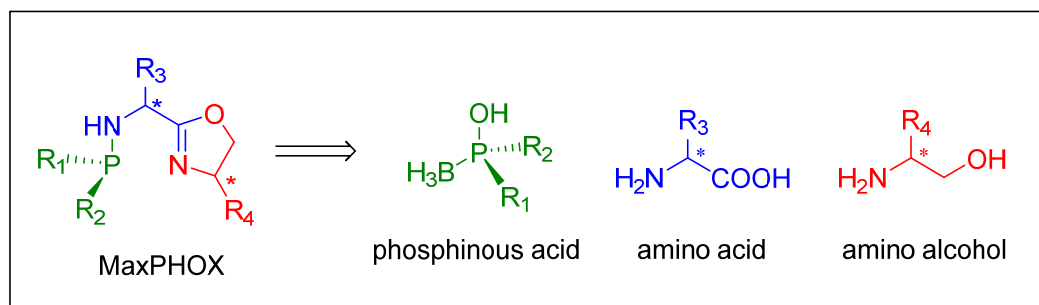


Figure 1: General structure of the MaxPHOX ligands.

We recently developed the MaxPHOX ligand system, which is built from three fragments—an amino alcohol, an amino acid and a P-stereogenic phosphinous acid (Figure 1).⁴ The Ir-MaxPHOX complexes have shown outstanding selectivity in the hydrogenation of cyclic enamides.⁵ One of the key advantages of the MaxPHOX ligand is the structural diversity arising from its possible configurations and substitution patterns, which can be adapted to a specific reaction. To demonstrate this versatility, here we report on the asymmetric hydrogenation of *N*-aryl imines using the Ir-MaxPHOX catalyst system. To study the influence of the stereogenic center of the phosphorus atom, non-P-stereogenic MaxPHOX ligands were also synthesized and evaluated in the asymmetric hydrogenation. We spotted a catalyst that hydrogenates *N*-aryl imines with up to 96% enantiomeric excess (ee) at atmospheric pressure of hydrogen (balloon). The putative imine-cyclometalated catalyst derivatives were also isolated, characterized by X-ray analysis and tested in the reaction.

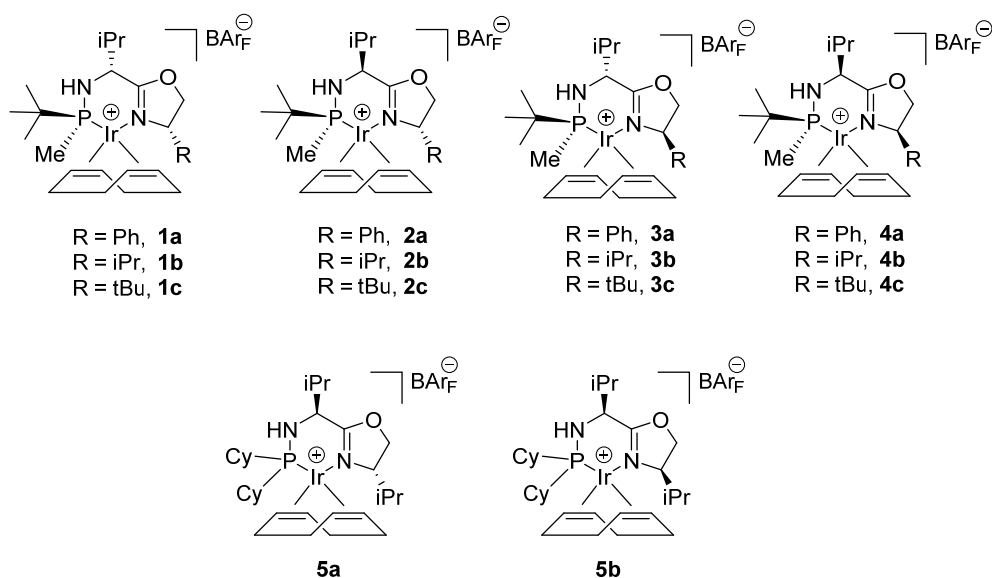


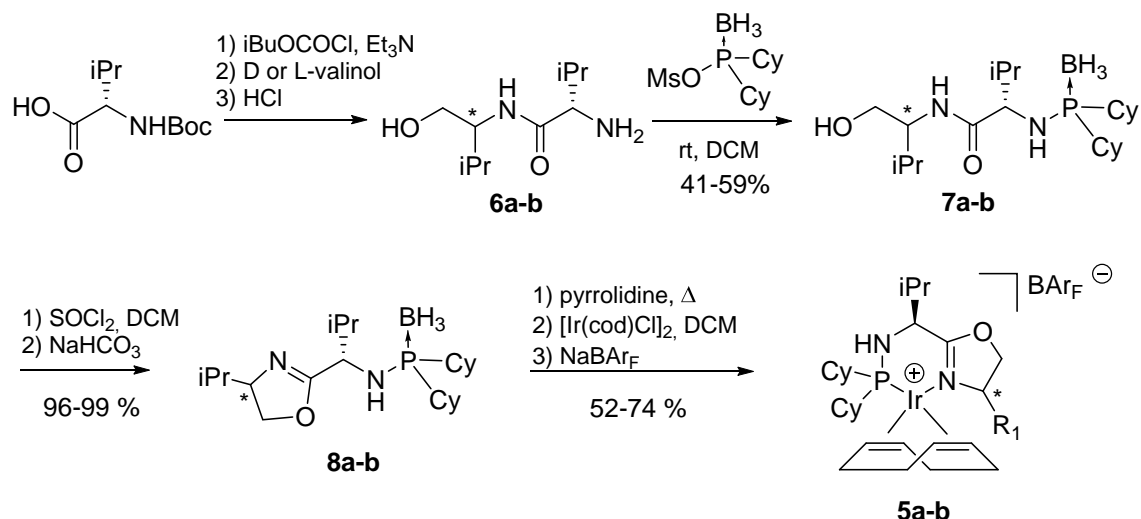
Figure 2: Ir-MaxPHOX catalysts used in the present study.

RESULTS AND DISCUSSION

Ligand Synthesis. The iridium catalysts used in the present study are shown in Figure 2. Twelve P-stereogenic MaxPHOX catalysts were employed. These arise from the four possible diastereomeric configurations **1**, **2**, **3** and **4**, plus three distinct oxazoline substitutions, R = Ph, (a), R = iPr (b), and R = tBu (c). The synthesis of these ligands (**1a-c**, **2a-c**, **3a-c** and **4a-c**) involved the coupling of amino acid, amino alcohol and P-stereogenic phosphinous acid fragments and final complexation with an iridium precursor.⁵ The corresponding non-P-stereogenic **5a** and **5b** ligands with a dicyclohexylphosphine moiety were also synthesized in a similar fashion, as shown in Scheme 1. *N*-Boc protected valine was coupled to either *D*- or *L*-valinol. The unprotected amino alcohols **6a-b** were then coupled to a phosphinyl mesyl mixed anhydride derived from dicyclohexylphosphinous acid borane.⁶ This reaction is highly selective for amine nucleophiles and it provided borane-protected aminophosphines **7a-b**. Reaction with SOCl₂ and treatment with NaHCO₃ gave the protected phosphine-oxazoline ligands **8a-**

b. Finally, borane deprotection with pyrrolidine, treatment with $[\text{Ir}(\text{cod})\text{Cl}]_2$, and counter ion exchange with NaBAr_F afforded non P-stereogenic catalysts **5a** and **5b** (Scheme 1).

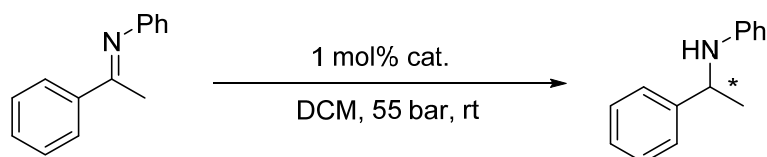
Scheme 1: Synthesis of non P-stereogenic Ir-MaxPHOX catalysts.



Asymmetric hydrogenation of imines. With the Ir-MaxPHOX catalysts in hand, we proceeded to study their performance in the hydrogenation of acetophenone *N*-phenyl imine with 1 mol% catalyst loading in DCM at 55 bar of H_2 (Table 1). The best results were obtained for catalysts with configurations **1** and **4**, the isopropyl group on the oxazoline providing the best results. Thus, complex **1b** gave the highest enantiomeric excess (89% ee) and **4b** the second best (85% ee) but with the opposite configuration. Catalysts **1b** and **4b** would be enantiomers of each other, except that the chirality at phosphorus is inverted. This result suggests that the stereochemical configuration at phosphorus had a limited impact on the selectivity. On the other hand, we observed that the configuration of the chiral center on the backbone of the ligand had a major effect on the selectivity. Catalysts **2b** and **3b**, while having the same configuration at the P-center and oxazoline with respect **1a** and **4b**, provided much lower selectivity. We called this

phenomenon the “tail effect”. We believe this behavior is associated with conformational changes within the Ir-P,N six-membered ring chelate. Finally, non P-stereogenic catalysts **5a** and **5b** were also tested, providing 57% and 81% ee, respectively. These results demonstrate that although the chiral oxazoline plays the most important role for our system, the presence of additional stereogenic centers both at the phosphine and the tail position is beneficial in terms of selectivity.

Table 1: Hydrogenation of acetophenone *N*-phenyl imine. Influence of the oxazoline substituent and the relative configuration of the catalysts.^a



R	P-stereogenic			
	1 (<i>S_PRS</i>)	2 (<i>S_PSS</i>)	3 (<i>S_PRR</i>)	4 (<i>S_PSR</i>)
Ph	60% ee 1a	12% ee 2a	43% ee 3a	47% ee 4a
<i>i</i> Pr	89% ee 1b	37% ee 2b	65% ee 3b	85% ee 4b
<i>t</i> Bu	79% ee 1c	53% ee 2c	53% ee 3c	77% ee 4c
	Non P-stereogenic			
<i>i</i> Pr		57% ee 5a		81% ee 5b

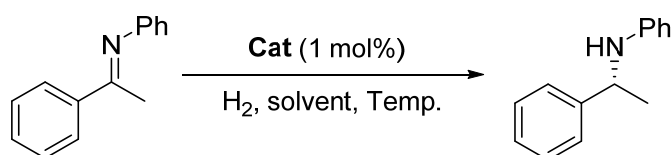
R	S	ee ^b (%)
		0-25
		25-50
		50-75
		75-100

a) All reactions were left to run overnight and went to 100% conversion as shown by ¹H NMR spectroscopy. b) Enantiomeric excess was determined by chiral HPLC.

With the best catalyst in hand (**1b**), we then studied the influence of hydrogen pressure, solvent and temperature on the reaction outcome (Table 2). Selectivity was relatively insensitive to the reaction pressure. In this regard, a reduction in the pressure from 55 bar to 3 bar produced only a slight increase in enantiomeric excess (from 89 to 90% ee, Table

2, entries 1 and 2). The pressure was even reduced to the atmospheric pressure of H₂ (balloon), giving the same results with respect to conversion and selectivity (Table 2, entry 3). Switching the reaction solvent from DCM to more coordinating solvents like EtOAc or MeOH caused a dramatic drop in selectivity (Table 2, entries 4 and 5). A reduction in reaction temperature enhanced selectivity. Thus at 0 °C and atmospheric H₂ pressure, the imine was reduced with 94% ee and lowering the temperature to –20 °C afforded the reduced amine with 96% ee (Table 2, entries 7 and 8). At this point, catalyst **4b** that only differs from the configuration at the P-center and which provided the second best selectivity (85% ee) in the initial catalysts screening at 55 bar, was also tested at atmospheric H₂ pressure (Table 2, entry 9). We observed that **4b** was considerably less active; since, after 72h, only 8% conversion was achieved. This demonstrates that while the chirality on phosphorous has a small influence on the selectivity it has a great impact on the catalyst activity.

Table 2: Optimization of reaction conditions. Influence of H₂ pressure, solvent and temperature.^a



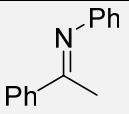
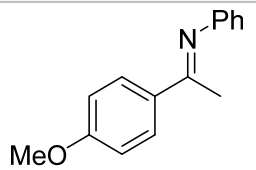
Entry	Cat	H ₂ (bar)	Solvent	Temp (°C)	Conv (%) ^b	ee (%) ^c
1	1b	55	DCM	rt	100	89
2	1b	3	DCM	rt	100	90
3	1b	balloon	DCM	rt	100	90
4	1b	3	EtOAc	rt	100	66
5	1b	3	MeOH	rt	100	45
6	1b	3	Toluene	rt	100	85
7	1b	balloon	DCM	0	100	94

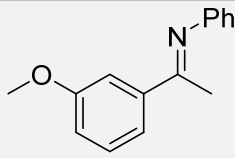
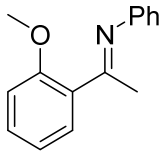
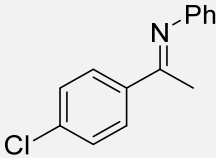
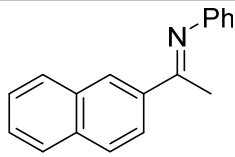
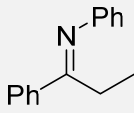
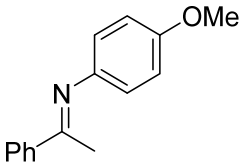
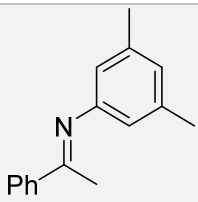
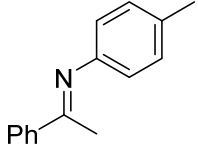
8	1b	balloon	DCM	−20	100	96
9 ^d	4b	balloon	DCM	rt	8	nd

a) All reactions were left to run overnight unless otherwise noted. b) Conversion was determined by ¹H NMR spectroscopy. c) Enantiomeric excess was determined by chiral HPLC. d) Reaction time 72h.

Once the reaction parameters had been optimized, we proceeded to assess the scope of the hydrogenation with catalyst **1b** with various aryl imines. Reduction of *p*- and *m*-methoxyacetophenone *N*-phenyl imine proceeded with 95% and 92% ee, respectively (Table 3, entries 2 and 3). However, *o*-methoxyacetophenone *N*-phenyl imine was hydrogenated with only 28% ee (Table 3, entry 4). This decrease in selectivity is most likely due to a less favorable E/Z ratio of the starting imine.⁷ *N*-Phenyl imines derived from *p*-chloroacetophenone and methyl 2-naphthyl ketone were both reduced, with 94% ee (Table 3, entries 5 and 6). Imine derived from ethyl phenyl ketone was also reduced, showing a lower enantiomeric excess (74%, Table 3, entry 7).⁷ Finally, acetophenone imines derived from other anilines, such as *p*-anisidine, *p*-toluidine and 2,3-dimethylaniline, were again reduced with excellent selectivity and with 90-95% ee.

Table 3: Hydrogenation of aryl amines with catalyst **1b**.^a

<u>Entry</u>	<u>Imine</u>	<u>Conv. (%)</u>	<u>ee (%)</u>
1		100	96
2		100	95

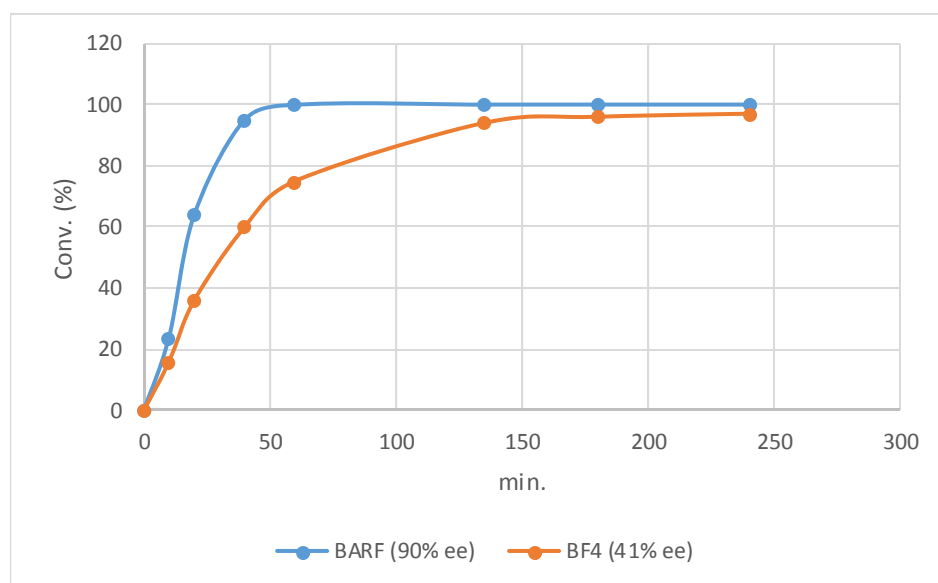
3		100	92
4		100	28
5		100	94
6 ^b		100	94
7 ^c		100	74
8		100	93
9		100	90
10		100	95

a) Unless specified all reactions were conducted overnight with 1 mol% catalyst loading in DCM at -20°C with atmospheric H_2 pressure (balloon). b) Reaction carried out with 2 mol% of catalyst loading at 3 bar of H_2 . c) Reaction conducted at room temperature.

Effect of the counter ion on the reaction rate, catalyst intermediates and mechanistic considerations. Since catalyst **1b** showed activity and selectivity that

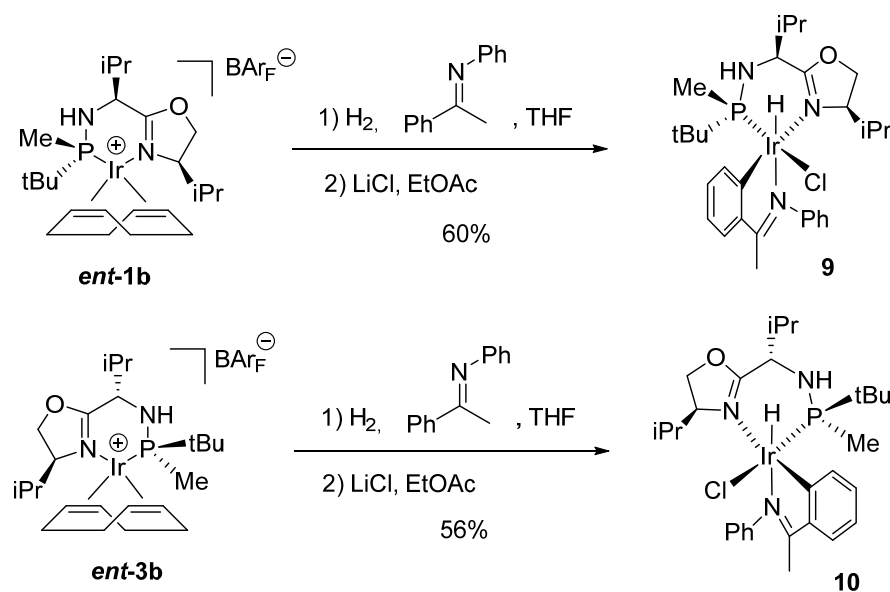
paralleled the best P,N-Ir systems reported for the hydrogenation of *N*-phenyl ketimines, we studied the rate of the reaction and how the counter ion influences the performance of the catalyst.⁸ The hydrogenation of acetophenone *N*-phenyl imine using 1 mol% of **1b**-**BAr_F** and **1b**-**BF₄** at atmospheric pressure of hydrogen was monitored by GC analysis, as shown in Figure 4. Catalyst **1b**-**BAr_F** proved extremely active, and 100% conversion was observed after 50 min using only atmospheric H₂ pressure. The use of a smaller counter ion, such as BF₄, resulted in a slower reaction and full conversion was only achieved after 150 min (2.5 h). Furthermore, the use of BF₄ as counter ion had a significant deleterious effect on selectivity since the product amine was obtained with only 41% ee (90% ee using BAr_F, Figure 3).

Figure 3: Conversion vs. reaction time graph for the hydrogenation of acetophenone *N*-phenyl imine using catalysts **1b** with BAr_F and BF₄ counter ions. Reactions were run at room temperature, 1 mol% catalyst loading, and atmospheric pressure of hydrogen in DCM.



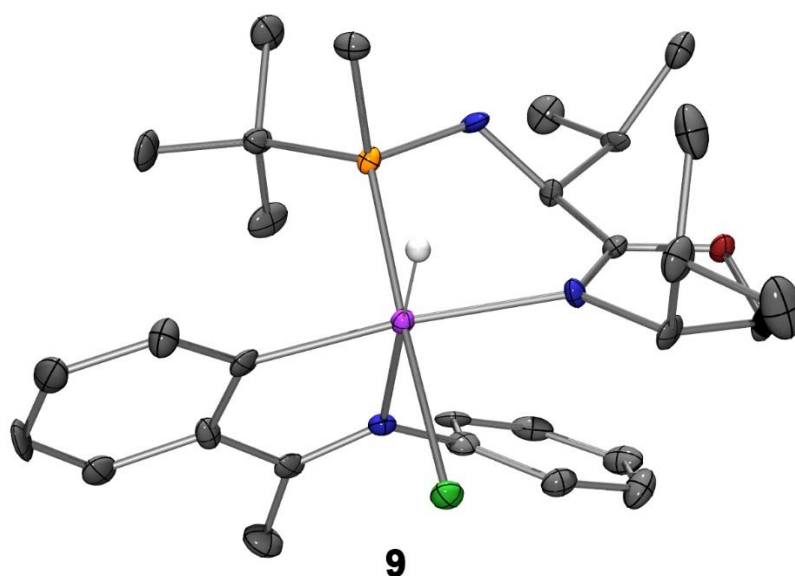
Pfaltz and coworkers have recently shown that an imine iridacycle is the actual catalyst when using Ir-P,N complexes.⁹ These cyclometallated Ir (III) species form spontaneously upon reaction between the iridium complex and the starting imine under hydrogen pressure. With this in mind, and to further increase knowledge of the true catalytic system, we questioned whether these intermediates are also involved in our Ir-MaxPHOX system. Complexes **1b** and **3b** were reacted under hydrogen atmosphere with acetophenone *N*-phenyl imine in THF (Scheme 2). Treatment of the reaction mixture with LiCl afforded the corresponding cyclometallated iridium hydride neutral complexes **9** and **10**.⁹ These complexes were isolated as a pale yellow solids by filtration on silica gel. ¹H and ³¹P NMR analysis confirmed compounds **9** and **10** as diastereomerically pure compounds. A single resonance for the Ir-H was observed at –19.76 ppm (d, $J_P = 26$ Hz) and –19.62 ppm (d, $J_P = 23$ Hz) for **9** and **10**, respectively. It should be noted that heteroleptic octahedral complexes such as **9** and **10** can, in principle, provide various diastereomers. It is therefore remarkable that in this case a single stereoisomer was generated.

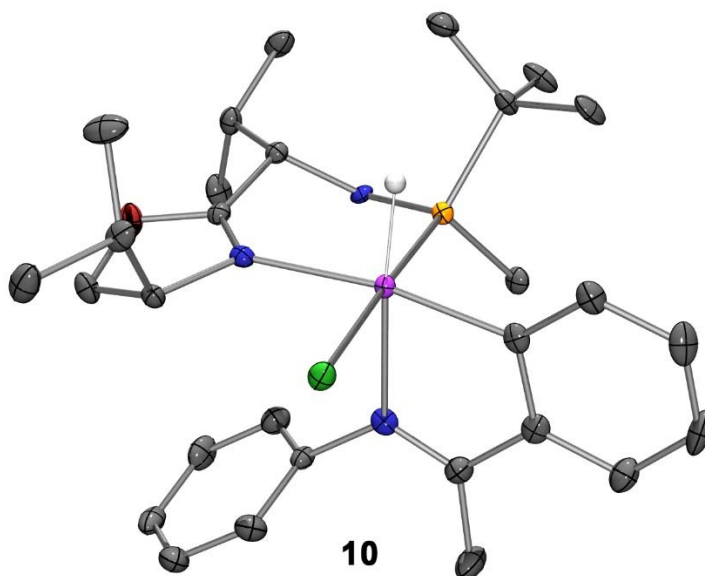
Scheme 2: Synthesis of iridacycles **9** and **10**.



To further characterize these species, compounds **9** and **10** were crystalized from hexane/DCM mixtures to obtain single crystals for X-ray analysis. The resulting solid state structures are shown in Figure 4. As expected, the iridium (III) displays octahedral coordination. The phosphino-oxazoline ligand and the cyclometallated imine ligand are perpendicular to each other, with the oxazoline nitrogen atom *trans* with respect the phenyl ring. The chiral center of the oxazoline fragment seems to control the coordination of the imine nitrogen. In both complexes, the C=N-Ph group is positioned away from the isopropyl substituent of the oxazoline ring. Finally, the hydride and chloride ligands are *cis* to each other and *trans* to the imine nitrogen and phosphine ligands respectively.

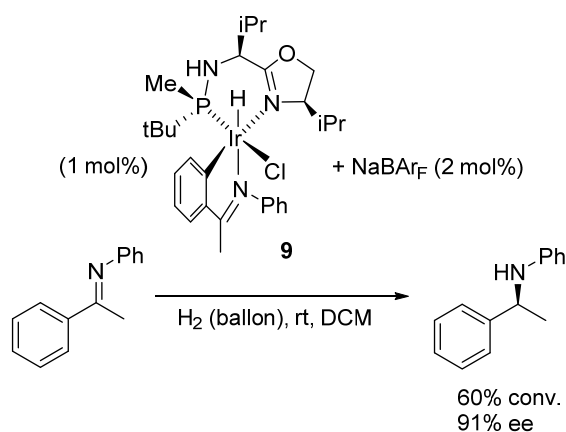
Figure 4: X-ray structures of iridacycles **9** and **10**. Ortep diagram shows ellipsoids at 50% probability. Only the hydrogen atom attached to iridium has been drawn.





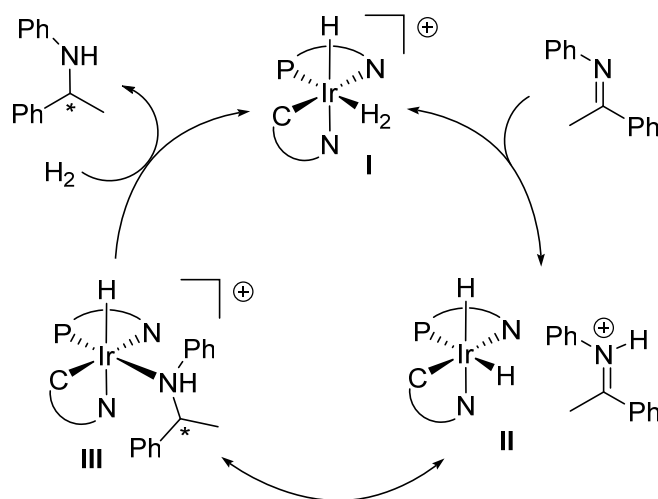
To verify whether the isolated imine iridacycles can be used as precatalysts, compound **9** was tested in the hydrogenation of imines. Thus, 1 mol% of **9** was treated with 2 equivalents of NaBAR_F in order to produce the active catalyst by counter ion exchange (Scheme 3). The use of this mixture as catalyst afforded the reduced product with 60% conversion and 91% ee. Despite the lower conversion observed, that can be justified by an inefficient chloride abstraction reaction, this result strongly suggests that the cationic cyclometallated complex arising from chloride abstraction of **9** is an active species in the catalytic cycle.

Scheme 3: The use of iridacycle **9** as precatalyst in the hydrogenation of imines.



For several years, the mechanism of imine reduction by iridium catalysts has been the subject of debate.¹⁰ During the preparation of this manuscript, Wiest and coworkers published a theoretical DFT mechanistic study of this process.¹¹ The authors took into account the findings of Pfaltz and considered cyclometalated iridium(III)-hydride species as the intermediates in the catalytic cycle. The study concluded that the hydrogenation with the cyclometalated precursors proceeds through an outer sphere mechanism, as depicted in a simplified manner in Scheme 4. According to this proposal, the active species in the catalytic cycle would be the cationic hydride-dihydrogen complex **I**, which, upon proton transfer, activates the imine to form the neutral dihydride complex **II**. The stereodetermining step is the hydride transfer *trans* to phosphorus to the activated imine to yield complex **III**.

Scheme 4: Outer sphere mechanism for the iridium-catalyzed hydrogenation of imines.

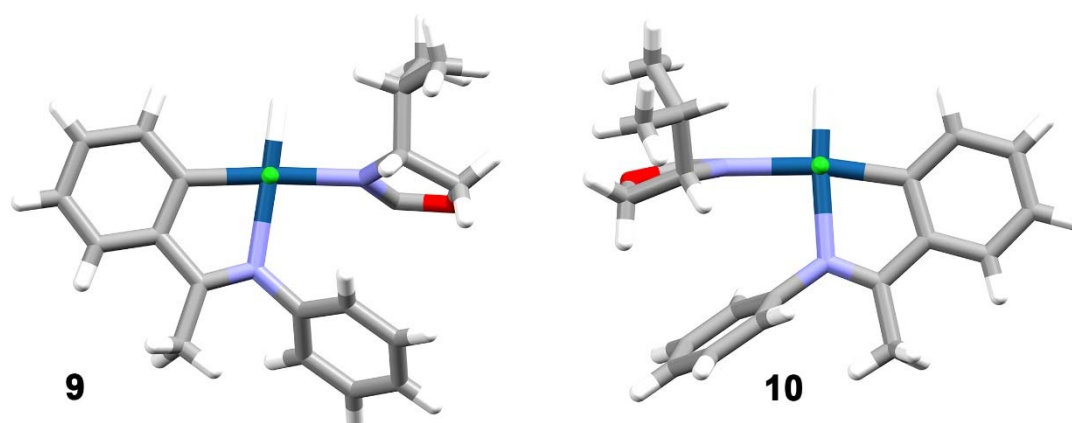


Our results are in agreement with this proposal. In this system, the imine ligand and the oxazoline isopropyl substituent are the fragments that surround the hydride transferred to the protonated imine in the stereodetermining step (Figure 5). Analyzing the selectivity observed with the four stereoisomers of MaxPHOX ligands (**1b**, **2b**, **3b** and **4b**, Table 1),

we can conclude that the chirality on phosphorus and the tail position is highly relevant. The intriguing question now is that since phosphine and the tail moiety are placed far away from the reacting center, why does the chirality on these fragments have such an impact on selectivity?

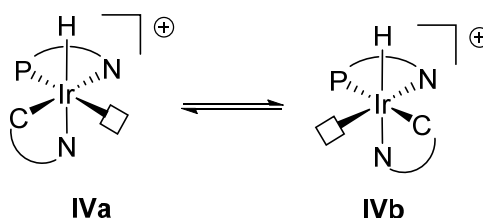
Two concurrent effects could explain this behavior. First, small conformational differences on the reacting site may provide a selectivity bias. Observing the *pseudo*-enantiomeric reacting sites (Figure 5) in complex **9**, the *N*-phenyl of the cyclometalated imine is tilted upwards, while for **10**, the *N*-phenyl ring is almost perpendicular to the Ir-imine metallacycle. These conformational differences of the *N*-phenyl group are ultimately governed by the configuration of the phosphine and tail positions and should lead to a difference in selectivity between **9** and **10**.¹²

Figure 5: Reacting sites for complexes **9** and **10** as extracted from the corresponding X-ray structures. The phosphine and ligand backbone have been deleted for clarity. View along the Cl-Ir bond axis (green dot). The green dot also corresponds to the hydride transferred in the stereodetermining step.



A second effect would be the relative stability of complexes **IVa/IVb** with a vacant coordination site (Scheme 5). It is easy to envisage that the coordination of H₂ to either complex **IVa** or **IVb** would provide a different selectivity outcome. Therefore, the stereochemical stability of the transient iridium complexes appears to be essential to guarantee high selectivity during hydrogenation. This notion is in agreement with the fact that in our case **9** and **10** have the stereochemistry of **IVa**, while Pfaltz and co-workers, reported the X-ray crystal structure of an [IrH(THF)(PHOX)(imine)]⁺ complex, where the cyclometalated phenyl group is *trans* to phosphine and which, upon removal of the solvent molecule, provides a complex with the same stereochemistry at the metal as **IVb**.⁹ We believe that the chirality on phosphorous and the tail positions in the MaxPHOX ligand system are important for stabilizing the arrangement of the ligands around the metal center in the true catalytic species.

Scheme 5: Equilibrium between complexes **IVa** and **IVb** with a vacant coordination site.



CONCLUSIONS

From a small family of P-stereogenic Ir-MaxPHOX precatalysts, we pinpointed complex **1b**, which shows activity and selectivity that matches the best Ir-P,N systems in the hydrogenation of acyclic imines. Catalyst **1b** hydrogenated *N*-aryl imines with up to 96% ee at atmospheric pressure of hydrogen and low temperature. Catalyst **4b** that only differs from the configuration at the P-center was significantly less active, demonstrating that the chirality on phosphorous has a great impact on the catalyst activity. Non-P-

stereogenic analogs of Ir-MaxPHOX were also synthesized and provided lower selectivity. The nature of the counter ion greatly influences the reaction outcome; smaller counter ions (e.g. BF_4) provided slower reactions and reduced enantiomeric excess. The active catalyst species are cationic iridium complexes that have an imine molecule from the substrate incorporated *via* cyclometalation. Cyclometalated $[\text{IrHCl}(\text{MaxPHOX})(\text{imine})]$ complexes **9** and **10** were isolated and characterized by X-ray crystallography. Chloride abstraction with NaBAr_F on **9** provided a functional catalytic system with the same level of selectivity as that obtained with catalyst **1b**. While the chirality of phosphorus and the tail position are away from the reacting center, they are non-innocent with respect to the performance of the catalyst. We propose that these moieties modify the reacting site by inducing small conformational differences on the *N*-phenyl ring of the cyclometalated imine and by stabilizing the relative arrangement of the imine and phosphine-oxazoline ligands around the iridium center.

EXPERIMENTAL SECTION

General methods. All reactions were carried out in dried solvents under nitrogen atmosphere. Et_2O and CH_2Cl_2 were dried in a purification system. Other commercially available reagents and solvents were used with no further purification. Thin layer chromatography was carried out using TLC-aluminum sheets with silica gel. Flash chromatography was performed by using an automated chromatographic system with hexane/ethyl acetate or hexane/dichloromethane gradients as eluent unless otherwise stated. NMR spectra were recorded at 23°C on a 400 MHz, 500 MHz or 600 MHz apparatus. ^1H NMR and ^{13}C NMR spectra were referenced either to relative internal TMS or to residual solvent peaks. ^{31}P NMR spectra were referenced to phosphoric acid. Optical rotations were measured at room temperature (25°C) and concentration is expressed in g/100 mL. Melting points were determined using a Büchi apparatus and were not

corrected. IR spectra were recorded in a FT-IR apparatus. HRMS were recorded in a LTQ-FT spectrometer using the Nanoelectrospray technique. Catalysts **1**, **2**, **3** and **4** were prepared as described previously.⁵

Dicyclohexyl phosphinous acid borane.⁶ In a N₂ purged round bottom flask 2g of chlorodicyclohexylphosphine (8.59 mmol, 1 eq) were weighed. Anhydrous THF (8 mL) was added and the reaction was cooled to 0 °C. Then, 815 µL (8.59 mmol, 1 eq) of BH₃.SMe₂ were added dropwise. The reaction was left stirring 1 hour at room temperature. Then it was cooled again to 0 °C and 2g (51.5 mmol, 6 eq) of NaOH solved in 32 mL of H₂O/THF (1/2) were slowly added. The solution was left stirring overnight at room temperature. Using a diluted solution of aqueous HCl, the reaction was quenched and brought to neutral pH. It was then extracted thrice with Et₂O. The organic layers were dried over MgSO₄ and concentrated on a rotary evaporator under reduced pressure. Purification by column chromatography (SiO₂, hexanes:EtOAc) yielded 1.67 g (85%) of the desired product as a white solid. ¹H NMR (400 MHz, CDCl₃) δ; 2.68 (br s, 1H), 1.92 – 1.68 (m, 12H), 1.56 – 1.40 (m, 2H), 1.40 – 1.20 (m, 8H), 0.97 – 0.01 (m, 3H, P–BH₃) ppm.

General procedure for the synthesis of aminophosphines (7a-b). A solution of dicyclohexylphosphinous acid borane (1 eq) and methansulfonic anhydride (1.2 eq) in CH₂Cl₂ (0.2M) was cooled to 0 °C. To this solution, anhydrous NEt₃ (2.5 eq) was slowly added, and the mixture was stirred 1 h at 0 °C. The corresponding amine (1.5 eq) was then added and the solution was stirred overnight at room temperature. Water was added and the mixture was allowed to warm to room temperature. The organic layer was separated and the aqueous phase was extracted twice with CH₂Cl₂. The combined extracts were washed with brine and concentrated under reduced pressure. Purification by flash

chromatography (SiO₂, hexanes:EtOAc) yielded the corresponding products as white solids.

(S)-2-((dicyclohexylphosphanyl)amino)-N-((S)-1-hydroxy-3-methylbutan-2-yl)-3-methylbutanamide borane (7a). White solid. Yield: 41% (150 mg). Mp: 200–201 °C. $[\alpha]_D$: –5.6 (c 0.53, CHCl₃). IR (KBr) ν_{\max} : 3297, 2918, 2386, 2343 and 1648 cm^{–1}. ¹H NMR (400 MHz, CDCl₃) δ : 5.9 (br d, J = 7 Hz, 1H), 3.75 – 3.60 (m, 3H), 3.52 (td, J = 10, 6 Hz, 1H), 2.77 (br s, 1H), 2.23 (dd, J = 10, 4 Hz, 1H), 1.95 – 1.60 (m, 14H), 1.43 – 1.15 (m, 10H), 0.99 (d, J = 4 Hz, 3H), 0.98 – 0.96 (m, 6H), 0.96 (d, J = 4 Hz, 3H), 0.78 – –0.07 (m, P–BH₃).ppm. ¹³C NMR (101 MHz, CDCl₃) δ : 174.3 (C), 63.9 (CH), 62.3 (CH), 57.7 (CH), 35.2 (d, J_P = 32 Hz, CH), 34.9 (d, J_P = 41 Hz, CH), 33.7 (d, J_P = 5 Hz, CH), 28.8 (CH), 26.8 – 25.2 (m, 10 x CH₂), 19.4 (CH₃), 19.0 (CH₃), 18.9 (CH₃), 18.7 (CH₃) ppm. ³¹P NMR (202 MHz, CDCl₃) δ : 73.3 – 71.1 (m, P–BH₃) ppm. HRMS (nanoESI-Orbi) m/z: [M + H]⁺ Calcd for C₂₂H₄₆O₂N₂BP 413.3463; Found 413.3458.

(S)-2-((dicyclohexylphosphanyl)amino)-N-((R)-1-hydroxy-3-methylbutan-2-yl)-3-methylbutanamide borane (7b). White solid. Yield: 59% (214 mg). Mp: 122–123 °C. $[\alpha]_D$: +25.0 (c 0.58, CHCl₃). IR (KBr) ν_{\max} : 3318, 2935, 2854, 2368 and 1652 cm^{–1}. ¹H NMR (400 MHz, CDCl₃) δ : 5.86 (br s, 1H), 3.72 – 3.65 (m, 3H), 3.41 (td, J = 10, 7 Hz, 1H), 2.78 (br s, 1H), 2.16 (br d, J = 8 Hz, 1H), 1.97 – 1.60 (m, 14H), 1.44 – 1.14 (m, 10H), 1.00 (d, J = 7 Hz, 3H), 0.99 – 0.93 (m, 9H), 0.72 – 0.08 (m, BH₃) ppm. ¹³C NMR (101 MHz, CDCl₃) δ : 174.5 (C), 63.7 (CH₂), 62.9 (d, J = 2 Hz, CH), 57.6 (CH), 35.1 (d, J_P = 43 Hz, CH), 34.9 (d, J_P = 36 Hz, CH), 33.4 (d, J = 6 Hz, CH), 28.8 (CH), 26.8 – 25.2 (m, 10 x CH₂), 19.6 (CH), 19.4 (CH), 19.0 (CH), 18.9 (CH) ppm. ³¹P NMR (202 MHz, CDCl₃) δ : 74.5 – 69.7 (m, P–BH₃) ppm. HRMS (nanoESI-Orbi) m/z: [M + H]⁺ Calcd for C₂₂H₄₆O₂N₂BP 413.3463; Found 413.3461.

General procedure for the synthesis of phosphino-oxazolines (8a-b). The corresponding aminophosphane (1 eq) was dissolved in CH₂Cl₂ (0.08 M) and SOCl₂ (2.4 eq) was added drop wise at 0 °C. The solution was stirred 4 h at room temperature. The solution was then cooled down to 0 °C and NaHCO₃ saturated aqueous solution was added slowly until pH 8-9. The mixture was left stirring for 15 min at room temperature. The two phases were separated and the aqueous phase was extracted twice with CH₂Cl₂. The combined organic layers were washed with brine. The organic layer was dried over MgSO₄ and concentrated on a rotary evaporator under reduced pressure. Purification by column chromatography (SiO₂, hexanes:EtOAc) yielded the desired products as white solids.

1,1-dicyclohexyl-*N*-((*S*)-1-((*S*)-4-isopropyl-4,5-dihydrooxazol-2-yl)-2-methylpropyl)phosphanamine borane (8a). White Solid. Yield: 96% (120 mg). Mp: 122–123 °C. [α]_D: –29.3 (c 0.53, CHCl₃). IR (KBr) ν_{max} : 3318, 2922, 2845, 2390, 2330 and 1666 cm^{–1}. ¹H NMR (400 MHz, CDCl₃) δ : 4.27 (t, 1H), 4.01 (t, *J* = 8 Hz, 1H), 3.94 – 3.76 (m, 2H), 2.26 (br d, *J* = 10 Hz, 1H), 1.99 – 1.59 (m, 14H), 1.47 – 1.16 (m, 10H), 1.01 (d, *J* = 7 Hz, 3H), 0.94 – 0.88 (m, 9H), 0.70 – 0.10 (m, 3H, BH₃) ppm. ¹³C NMR (101 MHz, CDCl₃) δ : 168.1 (C), 71.9 (CH), 70.9 (CH₂), 56.1 (d, *J* = 2 Hz, CH), 35.8 (d, *J_P* = 34 Hz, CH), 34.3 (d, *J_P* = 44 Hz, CH), 34.0 (d, *J* = 4 Hz, CH), 33.0 (CH), 26.9 – 25.2 (m, 10 x CH), 19.2 (CH₃), 18.5 (CH₃), 18.2 (CH₃), 18.1 (CH₃) ppm. ³¹P-NMR (202 MHz, CDCl₃) δ 73.0 – 71.2 (m, P-BH₃) ppm. HRMS (nanoESI-Orbi) *m/z*: [M + H]⁺ Calcd for C₂₂H₄₄ON₂BP 395.3357; Found 395.3350.

1,1-dicyclohexyl-*N*-((*S*)-1-((*R*)-4-isopropyl-4,5-dihydrooxazol-2-yl)-2-methylpropyl)phosphanamine borane (8b). White Solid. Yield: 99% (66 mg). Mp: 123.5–124.5 °C. [α]_D: +16.0 (c 0.31, CHCl₃). IR (KBr) ν_{max} : 3328, 2916, 2398, 2362 and 1667 cm^{–1}. ¹H NMR (400 MHz, CDCl₃) δ : 4.28 (dd, *J* = 9, 8 Hz, 1H), 3.97 – 3.73 (m,

3H), 2.14 (dd, $J = 10, 3$ Hz, 1H), 1.97 – 1.59 (m, 14H), 1.47 – 1.17 (m, 10H), 0.98 (d, $J = 7$ Hz, 3H), 0.96 – 0.91 (m, 6H), 0.89 (d, $J = 7$ Hz, 3H), 0.72 – 0.05 (m, 3H, BH₃) ppm. ¹³C NMR (101 MHz, CDCl₃) δ : 168.2 (C), 71.9 (CH), 70.4 (CH₂), 55.9 (CH), 35.7 (d, $J_P = 33$ Hz, CH), 34.3 (d, $J_P = 44$ Hz, CH), 33.8 (CH), 32.5 (CH), 27.0 – 25.1 (m, 10 x CH₂), 19.2 (CH₃), 18.4 (CH₃), 18.3 (CH₃), 18.1(CH₃).ppm. ³¹P NMR (202 MHz, CDCl₃) δ ; δ 73.6 – 72.0 (m, P-BH₃) ppm. HRMS (nanoESI-Orbi) m/z : [M + H]⁺ Calcd for C₂₂H₄₄ON₂BP 395.3357; Found 395.3349.

General procedure for the preparation of [Ir(P,N)(COD)]BAr_F complexes (5a-b).

The corresponding borane protected ligand (1 eq) was dissolved in freshly distilled pyrrolidine (0.06 M) and stirred for 16 h at 90 °C. Afterwards, pyrrolidine was removed *in vacuo*. When no pyrrolidine remained, the crude was further dried under vacuum for 30 min at 50 °C (the crude was under N₂ during all the procedure). A solution of [Ir(COD)(Cl)]₂ (0.5 eq) in CH₂Cl₂ (0.06 M) was added to the free ligand via cannula. The resulting mixture was stirred for 40 min at room temperature. NaBAr_F (1 eq) was then added and the solution was stirred 1 h more at room temperature. The resulting crude was filtered through a small plug of silica gel, (first washed with Et₂O) under N₂, eluting with hexanes:CH₂Cl₂ (50-100%). The orange fraction was collected and concentrated to yield the corresponding iridium complexes as deep orange solids.

[Ir(8a)(COD)]BAr_F (5a). Orange solid. Yield: 74% (145 mg). Mp: 167–168 °C. [α]_D: +46.9 (c 0.60, CHCl₃). IR (KBr) ν_{max} : 2929, 2855, 1628, 1276 and 1129 cm⁻¹. ¹H NMR (400 MHz, CDCl₃) δ ; ¹H NMR (400 MHz, Chloroform-*d*) δ 7.75 – 7.68 (m, 8H), 7.53 (br s, 4H), 4.84 – 4.75 (m, 1H), 4.55 – 4.47 (m, 2H), 4.26 (t, $J = 10$ Hz, 1H), 4.12 – 4.04 (m, 1H), 3.95 – 3.86 (m, 1H), 3.54 – 3.47 (m, 1H), 3.47 – 3.36 (m, 2H), 2.42 – 2.34 (m, 2H), 2.26 – 2.18 (m, 2H), 2.16 – 1.52 (m, 17H), 1.42 – 1.15 (m, 12H), 1.09 (d, $J = 7$ Hz, 3H), 1.02 (d, $J = 7$ Hz, 3H), 0.88 (d, $J = 7$ Hz, 3H), 0.82 (d, $J = 7$ Hz, 3H) ppm. ¹³C NMR (101

MHz, CDCl₃) δ ; 175.0 (C), 161.7 (q, $J_B = 50$ Hz, 4 x C), 134.8 (8 x CH), 129.5 – 128.3 (m, 8 x C), 124.5 (q, $J_F = 273$ Hz, 8 x CF₃), 117.40 (hept, $J_F = 4$ Hz, 4 x CH), 92.70 (d, $J_P = 11$ Hz, CH), 89.0 (d, $J_P = 13$ Hz, CH), 69.9 (CH), 69.2 (CH), 62.6 (CH), 59.9 (CH), 59.7 (CH), 41.1 (d, $J_P = 32$ Hz, CH), 38.2 (CH), 37.1 (d, $J_P = 33$ Hz, CH), 36.0 (CH₂), 31.9 (CH), 31.9 (CH₂), 29.6 – 25.6 (m, 12 x CH₂), 20.6 (CH₃), 19.9 (CH₃), 18.6 (CH₃), 15.1 (CH₃) ppm. ³¹P NMR (202 MHz, CDCl₃) δ ; 60.7 (s) ppm. HRMS (nanoESI-Orbi) m/z: [M]⁺ Calcd for C₃₀H₅₃ON₂IrP 681.3519; Found 681.3502. HRMS (nanoESI-Orbi) m/z: [M][−] Calcd for C₃₂H₁₂BF₂₄ 863.0654; Found 863.0634.

[Ir(8b)(COD)]BAr_F (5b). Orange solid. Yield: 52% (102 mg). [α]_D: −41.2 (c 0.49, CHCl₃). IR (KBr) ν_{max} : 2940, 2856, 1622, 1351 and 1271 cm^{−1}. ¹H NMR (400 MHz, CDCl₃) δ ; 7.74 – 7.67 (m, 8H), 7.53 (br s, 4H), 4.80 – 4.73 (m, 1H), 4.61 (p, $J = 7$ Hz, 1H), 4.54 (dd, $J = 10, 4$ Hz, 1H), 4.28 (t, $J = 10$ Hz, 1H), 4.05 – 3.99 (m, 1H), 3.90 (dt, $J = 10, 3$ Hz, 1H), 3.82 – 3.76 (m, 1H), 3.39 – 3.31 (m, 1H), 2.52 – 1.16 (m, 33H), 1.11 (d, $J = 7$ Hz, 3H), 0.93 (d, $J = 7$ Hz, 3H), 0.92 (d, $J = 7$ Hz, 3H), 0.74 (d, $J = 7$ Hz, 3H) ppm. ¹³C NMR (101 MHz, CDCl₃) δ ; 175.0 (C), 161.7 (q, $J_B = 50$ Hz, 4 x C), 134.8 (8 x CH), 129.5 – 128.3 (m, 8 x C), 124.5 (q, $J_F = 273$ Hz, 8 x CF₃), 117.40 (hept, $J_F = 4$ Hz, 4 x CH), 93.8 (d, $J_P = 12$ Hz, CH), 92.0 (CH), 70.3 (CH₂), 68.4 (CH), 61.7 (CH), 60.1 (CH), 58.7 (CH), 39.7 (d, $J_P = 37$ Hz, CH), 37.6 (d, $J_P = 29$ Hz, CH), 35.3 (CH₂), 31.8 (CH), 30.9 – 25.5 (m, 13 x CH₂ and 1 x CH), 20.1 (CH₃), 18.9 (CH₃), 16.2 (CH₃), 14.2 (CH₃) ppm. ³¹P NMR (202 MHz, CDCl₃) δ ; 59.7 (s) ppm. HRMS (nanoESI-Orbi) m/z: [M]⁺ Calcd for C₃₀H₅₃ON₂IrP 681.3519; Found 681.3501. HRMS (nanoESI-Orbi) m/z: [M][−] Calcd for C₃₂H₁₂BF₂₄ 863.0654; Found 863.0654.

[Ir(P*,N)(COD)]BF₄ (1b-BF₄). 45 mg of (*R*)-1-*tert*-butyl-N-((*R*)-1-((*S*)-4-(isopropyl)-4,5-dihydrooxazol-2-yl)-2-methylpropyl)-1-methylphosphanamine borane (0.148 mmol, 1 eq) was dissolved in freshly distilled pyrrolidine (0.06 M) and stirred for

16 h at 90 °C. Afterwards pyrrolidine was removed *in vacuo*. When no pyrrolidine remained, the crude was further dried under vacuum for 30 min at 50 °C (the crude was under N₂ during all the procedure). 50 mg of [Ir(COD)(Cl)]₂ (0.074 mmol, 0.5 eq) in CH₂Cl₂ (2 mL) were added to the free ligand. The resulting mixture was stirred for 40 min at room temperature. Then, 17 mg of NaBF₄ (0.148 mmol, 1 eq) were added and the solution was left stirring overnight at room temperature. Purification by flash chromatography (SiO₂, DCM:MeOH) yielded 63 mg (63%) of product as an orange/red solid. Mp: 200–202 °C. [α]_D: –18.5 (c 0.40, CHCl₃). IR (KBr) ν_{max} : 3346, 2956, 2874, 1620 and 1213 cm^{–1}. ¹H NMR (400 MHz, CDCl₃) δ : 5.11 – 5.02 (m, 1H), 4.91 – 4.84 (m, 1H), 4.69 (t, *J* = 10 Hz, 1H), 4.56 (dd, *J* = 10, 4 Hz, 1H), 4.19 – 4.13 (m, 1H), 4.02 (dt, *J* = 10, 4 Hz, 1H), 3.63 – 3.57 (m, 1H), 3.57 – 3.46 (m, 1H), 2.63 – 2.53 (m, 1H), 2.53 – 2.42 (m, 1H), 2.39 – 2.17 (m, 3H), 2.16 – 2.06 (m, 2H), 1.84 – 1.65 (m, 4H), 1.42 (d, *J*_P = 8 Hz, 3H), 1.22 (d, *J*_P = 15 Hz, 9H), 1.10 (d, *J* = 7 Hz, 3H), 1.01 (d, *J* = 7 Hz, 3H), 0.98 (d, *J* = 7 Hz, 3H), 0.79 (d, *J* = 7 Hz, 3H) ppm. ¹³C NMR (101 MHz, CDCl₃) δ : 175.7 (C), 95.1 (d, *J*_P = 13 Hz, CH), 92.8 (d, *J*_P = 11 Hz, CH), 70.8 (CH₂), 68.5 (CH), 64.0 (CH), 57.9 (CH), 56.1 (CH), 36.3 (d, *J*_P = 42 Hz, C), 34.3 (CH₂), 31.8 (CH), 31.3 (CH₂), 29.8 (CH₂), 28.9 (d, *J*_P = 9 Hz, CH), 28.0 (CH₂), 26.9 (d, *J* = 4 Hz, 3 x CH₃), 19.8 (CH₃), 19.3 (CH₃), 17.1 (CH₃), 15.1 (CH₃), 8.7 (d, *J*_P = 27 Hz, CH₃) ppm. ³¹P NMR (202 MHz, CDCl₃) δ : 61.9 (s) ppm. HRMS (nanoESI-Orbi) *m/z*: [M]⁺ Calcd for C₂₃H₄₃ON₂IrP 587.2737; Found 587.2721. HRMS (nanoESI-Orbi) *m/z*: [M][–] Calcd for BF₄ 87.0035; Found 87.0034.

General procedure for the synthesis of imines. The corresponding ketone (1 eq) was dissolved in a dry, N₂ purged round bottom flask in anhydrous Et₂O (0.5 M). Then the corresponding amine (3 eq) was added. The mixture was cooled to 0 °C. Then neat TiCl₄ (0.5 eq) was carefully added dropwise via syringe. The reaction was left stirring overnight

at room temperature. The solution was then filtered through Celite® with extra Et₂O. The solvent was then removed under reduced pressure to obtain the crude as an oil. The crudes were purified by either crystallization or Kugelrohr distillation.

Acetophenone *N*-phenyl imine.^{3a} Yield: 73% (10.9 g). ¹H NMR (400 MHz, CDCl₃) δ; 8.02 – 7.91 (m, 2H), 7.55 – 7.40 (m, 3H), 7.41 – 7.30 (m, 2H), 7.13 – 7.04 (m, 1H), 6.84 – 6.76 (m, 2H), 2.23 (s, 3H) ppm.

4-Methoxyacetophenone *N*-phenyl imine.^{3a} Yield: 63% (9.5 g). ¹H NMR (400 MHz, CDCl₃) δ; 8.04 – 7.92 (m, 2H), 7.39 – 7.31 (m, 2H), 7.10 – 7.04 (m, 1H), 6.98 – 6.93 (m, 2H), 6.82 – 6.76 (m, 3H), 3.87 (s, 3H), 2.20 (s, 3H) ppm.

3-Methoxyacetophenone *N*-phenyl imine.¹³ Yield: 38% (5.7 g). ¹H NMR (400 MHz, CDCl₃) δ; 7.61 – 7.54 (m, 1H), 7.53 – 7.48 (m, 1H), 7.39 – 7.31 (m, 3H), 7.11 – 7.06 (m, 1H), 7.04 – 7.00 (m, 1H), 6.81 – 6.77 (m, 2H), 3.88 (s, 3H), 2.22 (s, 3H) ppm.

2-Methoxyacetophenone *N*-phenyl imine. Yield: 33% (5.4 g). ¹H NMR (400 MHz, CDCl₃) δ; 7.61 – 7.57 (m, 1H), 7.41 – 7.32 (m, 3H), 7.04 – 7.00 (m, 1H), 6.97 – 6.93 (m, 1H), 6.87 – 6.84 (m, 2H), 6.78 – 6.73 (m, 1H), 6.68 – 6.64 (m, 1H), 3.88 (s, 3H), 2.19 (s, 3H) ppm.

Acetophenone *N*-(4-methoxyphenyl) imine.^{3a} Yield: 55% (5.3 g). ¹H NMR (400 MHz, CDCl₃) δ; 8.03 – 7.89 (m, 2H), 7.50 – 7.39 (m, 3H), 6.93 – 6.87 (m, 2H), 6.80 – 6.72 (m, 2H), 3.82 (s, 3H), 2.25 (s, 3H) ppm.

1-(Naphthalen-2-yl)-*N*-phenylethan-1-imine.¹⁴ Yield: 62% (5.4 g). ¹H NMR (400 MHz, CDCl₃) δ; 8.37 – 8.33 (m, 1H), 8.24 – 8.21 (m, 1H), 7.95 – 7.85 (m, 3H), 7.57 – 7.49 (m, 2H), 7.40 – 7.34 (m, 2H), 7.13 – 7.08 (m, 1H), 6.87 – 6.82 (m, 2H), 2.36 (s, 3H) ppm.

N,1-Diphenylpropan-1-imine.^{3a} Yield: 47% (3.7 g). ¹H NMR (400 MHz, CDCl₃) δ; 7.95 – 7.90 (m, 2H), 7.48 – 7.42 (m, 3H), 7.37 – 7.31 (m, 2H), 7.07 (tt, *J* = 8, 1 Hz, 1H), 6.81 – 6.77 (m, 2H), 2.66 (q, *J* = 8 Hz, 2H), 1.08 (t, *J* = 8 Hz, 3H) ppm.

4-Chloroacetophenone N-phenyl imine.^{3a} Yield: 51% (9.0 g). ¹H NMR (400 MHz, CDCl₃) δ; 7.94 – 7.88 (m, 2H), 7.43 – 7.38 (m, 2H), 7.38 – 7.32 (m, 2H), 7.12 – 7.06 (m, 1H), 6.81 – 6.76 (m, 2H), 3.08 (q, *J* = 7 Hz, 1H), 2.21 (s, 3H), 1.40 (t, *J* = 7 Hz, 1H) ppm.

Acetophenone N-(3,5-dimethylphenyl) imine.¹⁵ Yield: 57% (7.1 g). ¹H NMR (400 MHz, CDCl₃) δ; 7.98 – 7.94 (m, 2H), 7.48 – 7.40 (m, 3H), 6.72 (tp, *J* = 1, 1 Hz, 1H), 6.44 – 6.40 (m, 2H), 2.32 – 2.30 (m, 6H), 2.23 (s, 3H) ppm.

Acetophenone N-(*p*-tolyl) imine.¹⁶ Yield: 40% (7.2 g). ¹H NMR (400 MHz, CDCl₃) δ; 8.01 – 7.92 (m, 2H), 7.48 – 7.41 (m, 3H), 7.18 – 7.14 (m, 2H), 6.73 – 6.67 (m, 2H), 2.35 (s, 3H), 2.24 (s, 3H) ppm.

General Procedure for the hydrogenation at high H₂ pressure. The corresponding imine (1 eq) and the corresponding catalyst (0.01 eq) were placed along with stirring bar in a glass tube inside a stainless steel high pressure reactor. The reactor was entered into a glove box and deoxygenated anhydrous solvent was added (0.17 M). The reactor was closed, removed from the glove box and connected to a hydrogen manifold. While stirring, the reactor was purged with vacuum-hydrogen cycles and then it was charged at the designated pressure. The hydrogen manifold was unplugged and the mixture was left to stir overnight at room temperature. The reactor was depressurized and the reaction was concentrated under vacuum. The conversion was determined by ¹H NMR. Catalyst was removed by filtration of the crude reaction through a short silica pad with CH₂Cl₂ and concentrated under vacuum. At this point, yield and enantiomeric excess were determined.

General Procedure for the hydrogenation at atmospheric H₂ pressure. The corresponding imine (1 eq) and the corresponding catalyst (0.01 eq) were placed in a round bottom flask. The flask was purged with N₂ and deoxygenated anhydrous solvent was added (0.17 M). The reaction was then set at the desired temperature. While stirring, a H₂ filled balloon was connected. Using another needle as a gas exit the round bottom flask was purged with H₂ until the solution went from orange to yellow (usually less than 3-4 minutes). The gas exit was removed and the reaction was left stirring overnight. The next day the reaction was concentrated under vacuum. The conversion was determined by ¹H NMR. Catalyst was removed by filtration of the crude reaction through a short silica pad with CH₂Cl₂ and concentrated under vacuum. At this point, yield and enantiomeric excess were determined.

***N*-(1-phenylethyl)aniline.**^{3a} Yield: 97% (66 mg). ¹H NMR (400 MHz, CDCl₃) δ; 7.41 – 7.25 (m, 4H), 7.28 – 7.18 (m, 1H), 7.18 – 7.03 (m, 2H), 6.68 – 6.59 (m, 1H), 6.55 – 6.46 (m, 2H), 4.48 (q, *J* = 7 Hz, 1H), 4.02 (br s, 1H), 1.51 (dd, *J* = 7, 1 Hz, 3H) ppm. HPLC: CHIRALCEL OD-H. Heptane/*i*-PrOH 90:10, 1 mL/min, λ = 220 nm. *t_R*(+)= 15.4 min, *t_R*(–)= 17.0 min. (*ee* = 96%).

***N*-(1-(4-methoxyphenyl)ethyl)aniline.**^{3a} Yield: 96% (76 mg). ¹H NMR (400 MHz, CDCl₃) δ; 7.30 – 7.26 (m, 2H), 7.11 – 7.06 (m, 2H), 6.87 – 6.84 (m, 2H), 6.53 – 6.47 (m, 2H), 4.44 (q, *J* = 6.7 Hz, 1H), 3.78 (s, 3H), 1.49 (d, *J* = 6.7 Hz, 3H) ppm. HPLC: Chiralpak IA. Heptane/*i*-PrOH 96:4, 0.5 mL/min, λ = 210 nm. *t_R*(+)= 16.1 min, *t_R*(–)= 17.6 min. (*ee* = 95%).

***N*-(1-(3-methoxyphenyl)ethyl)aniline.**¹³ Yield: 98% (77 mg). ¹H NMR (400 MHz, CDCl₃) δ; 7.26 – 7.21 (m, 1H), 7.11 – 7.05 (m, 2H), 6.98 – 6.94 (m, 1H), 6.94 – 6.91 (m, 1H), 6.76 (ddd, *J* = 8, 3, 1 Hz, 1H), 6.64 (tt, *J* = 7, 1 Hz, 1H), 6.54 – 6.48 (m, 2H), 4.45 (q, *J* = 7 Hz, 1H), 4.01 (s, 1H), 3.78 (s, 3H), 1.51 (d, *J* = 7 Hz, 3H) ppm. HPLC:

CHIRALCEL OJ. Heptane/EtOH 50:50-0.2% DEA, 0.5 mL/min, $\lambda = 210$ nm. $t_R(+)$ = 18.1 min, $t_R(-)$ = 20.8 min. ($ee = 92\%$).

***N*-(1-(2-methoxyphenyl)ethyl)aniline.**¹⁷ Yield: 96% (75 mg). ¹H NMR (400 MHz, CDCl₃) δ ; 7.27 – 7.20 (m, 1H), 7.15 – 7.08 (m, 1H), 7.03 – 6.96 (m, 2H), 6.83 – 6.77 (m, 2H), 6.54 (tt, $J = 7$, 1 Hz, 1H), 6.46 – 6.37 (m, 2H), 4.77 (q, $J = 7$ Hz, 1H), 3.82 (s, 3H), 1.40 (d, $J = 7$ Hz, 3H) ppm. HPLC: CHIRALCEL OJ. Heptane/EtOH 70:30-0.2% DEA, 0.5 mL/min, $\lambda = 210$ nm. $t_R(+)$ = 14.5 min, $t_R(-)$ = 19.1 min. ($ee = 28\%$).

4-methoxy-*N*-(1-phenylethyl)aniline.^{3a} Yield: 98% (77 mg). ¹H NMR (400 MHz, CDCl₃) δ ; 7.39 – 7.28 (m, 4H), 7.24 – 7.19 (m, 1H), 6.74 – 6.61 (m, 2H), 6.47 (d, $J = 9$ Hz, 2H), 4.41 (q, $J = 7$ Hz, 1H), 3.69 (s, 3H), 1.50 (d, $J = 7$ Hz, 3H) ppm. HPLC: Chiralpak IC Heptane/*i*-PrOH 96:4, 0.5 mL/min, $\lambda = 210$ nm. $t_R(+)$ = 17.3 min, $t_R(-)$ = 18.4 min. ($ee = 93\%$).

***N*-(1-(naphthalen-2-yl)ethyl)aniline.**¹⁸ Yield: 96% (82 mg). ¹H NMR (400 MHz, CDCl₃) δ ; 7.84 – 7.77 (m, 4H), 7.50 (dd, $J = 8$, 2 Hz, 1H), 7.48 – 7.39 (m, 2H), 7.13 – 7.03 (m, 2H), 6.66 – 6.59 (m, 1H), 6.59 – 6.53 (m, 2H), 4.64 (q, $J = 7$ Hz, 1H), 4.18 – 4.04 (m, 1H), 1.59 (d, $J = 7$ Hz, 3H) ppm. HPLC: CHIRALCEL OJ. Heptane/EtOH 50:50, 0.8 mL/min, $\lambda = 210$ nm. $t_R(+)$ = 14.4 min, $t_R(-)$ = 17.2 min. ($ee = 94\%$).

***N*-(1-phenylpropyl)aniline.**^{3a} Yield: 99% (72 mg). ¹H NMR (400 MHz, CDCl₃) δ ; 7.39 – 7.27 (m, 4H), 7.27 – 7.18 (m, 1H), 7.11 – 7.04 (m, 2H), 6.62 (tt, $J = 7$, 1 Hz, 1H), 6.56 – 6.43 (m, 2H), 4.22 (t, $J = 7$ Hz, 1H), 4.04 (br s, 1H), 1.90 – 1.72 (m, 2H), 0.95 (t, $J = 7$ Hz, 3H) ppm. HPLC: CHIRALCEL OD-H. Heptane/*i*-PrOH 95:5, 0.5 mL/min, $\lambda = 210$ nm. $t_R(+)$ = 11.9 min, $t_R(-)$ = 14.8 min. ($ee = 74\%$).

***N*-(1-(4-chlorophenyl)ethyl)aniline.**^{3a} Yield: 98% (78 mg). ¹H NMR (400 MHz, CDCl₃) δ ; 7.25 – 7.18 (m, 4H), 7.05 – 6.97 (m, 2H), 6.62 – 6.54 (m, 1H), 6.43 – 6.35 (m, 2H), 4.38 (q, $J = 7$ Hz, 1H), 1.42 (d, $J = 7$ Hz, 3H) ppm. HPLC: CHIRALCEL OD-H.

Heptane/*i*-PrOH 95:5, 1 mL/min, λ = 210 nm. $t_R(+)$ = 10.4 min, $t_R(-)$ = 14.8 min. (*ee* = 94%).

3,5-dimethyl-*N*-(1-phenylethyl)aniline.¹⁹ Yield: 99% (77 mg). ¹H NMR (400 MHz, CDCl₃) δ ; 7.38 – 7.28 (m, 3H), 7.24 – 7.19 (m, 1H), 6.32 – 6.27 (m, 1H), 6.18 – 6.10 (m, 2H), 4.47 (q, *J* = 7 Hz, 1H), 3.90 (br s, 1H), 2.16 (s, 6H), 1.49 (d, *J* = 7 Hz, 3H) ppm. HPLC: CHIRALCEL OD-H. Heptane/*i*-PrOH 95:5, 0.5 mL/min, λ = 254 nm. $t_R(+)$ = 10.7 min, $t_R(-)$ = 12.4 min. (*ee* = 90%).

4-methyl-*N*-(1-phenylethyl)aniline.²⁰ Yield: 96% (70 mg). ¹H NMR (400 MHz, CDCl₃) δ ; 7.38 – 7.28 (m, 4H), 7.24 – 7.19 (m, 1H), 6.94 – 6.84 (m, 2H), 6.47 – 6.39 (m, 2H), 4.45 (q, *J* = 7 Hz, 1H), 2.18 (s, 3H), 1.50 (d, *J* = 7 Hz, 3H) ppm. HPLC: CHIRALCEL OJ. Heptane/*i*-PrOH 50:50, 1 mL/min, λ = 210 nm. $t_R(+)$ = 12.2 min, $t_R(-)$ = 15.4 min. (*ee* = 95%).

General Procedure for synthesis of imine iridacycles. In a round bottom flask 100 mg of complex **ent-1b** or **ent-3b** (0.069 mmol, 1 eq) and 27 mg of acetophenone *N*-phenyl imine (0.138 mmol, 2 eq) were placed. The flask was then purged with N₂ and THF (2 mL) was added. The solution was purged with a balloon of H₂ until the orange color changed to yellow. The reaction mixture was stirred at room temperature during 4 hours. The solvent was removed with a N₂ flow and LiCl (100 mg), SiO₂ (100 mg) and EtOAc (2 mL) were added. The reaction was left to stir overnight. The solvent was again removed with a N₂ flow. The crude was suspended in pentane/TBME (1:1) and eluted through SiO₂. Only the yellow colored band was collected affording the desired products. The complexes were crystalized with hexanes/DCM to obtain single crystals for X-ray analysis.

[IrHCl(P*,N)(imine)] (9). Yellow solid. Yield: 60% (29 mg). ¹H NMR (400 MHz, CD₂Cl₂) δ ; 7.80 – 7.68 (m, 2H), 7.57 – 7.50 (m, 1H), 7.40 – 7.30 (m, 2H), 7.17 (tt, *J* = 7,

1 Hz, 1H), 6.96 – 6.91 (m, 3H), 5.02 – 4.96 (m, 1H), 4.30 (dd, $J = 9, 5$ Hz, 1H), 3.98 (dd, $J = 10, 9$ Hz, 1H), 3.01 – 2.93 (m, 1H), 2.74 – 2.65 (m, 1H), 2.41 (s, 3H), 1.86 (dd, $J = 9, 1$ Hz, 3H), 1.84 – 1.78 (m, 1H), 1.12 (br d, $J = 10$ Hz, 1H), 0.86 (d, $J = 7$ Hz, 3H), 0.81 (d, $J = 7$ Hz, 3H), 0.78 (d, $J = 7$ Hz, 3H), 0.64 (d, $J = 7$ Hz, 3H), 0.57 (d, $J_P = 14$ Hz, 9H), -19.76 (d, $J_{P(cis)} = 26$ Hz, 1H) ppm. ^{13}C NMR (101 MHz, CD_2Cl_2) δ ; 180.0 (C), 168.5 (C), 155.6 – 154.2 (m, C), 149.5 (C), 148.4 (C), 143.2 (d, $J = 1$ Hz, CH), 130.6 (CH), 129.2 (CH), 128.4 – 127.7 (m, 2 x CH), 125.5 (CH), 123.6 (CH), 121.9 (CH), 119.8 (CH), 68.8 (CH₂), 67.5 (CH), 57.5 (d, $J = 2$ Hz, CH), 37.4 (d, $J_P = 37$ Hz, C), 28.1 (d, $J = 8$ Hz, CH), 27.8 (CH), 25.8 (d, $J = 4$ Hz, 3 x CH₃), 22.3 – 21.3 (m, CH₃), 20.1 (CH₃), 18.2 (CH₃), 17.6 (CH₃), 16.8 (CH₃), 13.4 (CH₃) ppm. ^{31}P NMR (202 MHz, CDCl_3) δ ; 36.3 (d, $J_H = 20$ Hz) ppm. HRMS (nanoESI-Orbi) m/z : $[\text{M} - \text{Cl}]^+$ Calcd for $\text{C}_{29}\text{H}_{44}\text{IrN}_3\text{OP}$ 674.2846; Found 674.2834.

[IrHCl(P*,N)(imine)] (10). Yellow solid. Yield: 56% (27 mg). ^1H NMR (400 MHz, CD_2Cl_2) δ ; 7.85 – 7.56 (m, 2H), 7.51 – 7.48 (m, 1H), 7.41 – 7.26 (m, 2H), 7.15 (tt, $J = 8, 1$ Hz, 1H), 7.01 – 6.74 (m, 3H), 4.93 (dtd, $J = 9, 3, 1$ Hz, 1H), 4.20 (dd, $J = 9, 3$ Hz, 1H), 3.73 – 3.68 (m, 1H), 3.65 (dd, $J = 9, 9$ Hz, 1H), 2.89 (hd, $J = 7, 3$ Hz, 1H), 2.35 (s, 3H), 2.07 – 1.95 (m, 1H), 1.55 – 1.49 (m, 1H), 1.07 (d, $J_P = 15$ Hz, 9H), 0.90 (d, $J_P = 9$ Hz, 3H), 0.86 (d, $J = 7$ Hz, 3H), 0.77 (d, $J = 7$ Hz, 3H), 0.63 (d, $J = 7$ Hz, 3H), 0.43 (d, $J = 7$ Hz, 3H), -19.62 (d, $J_{P(cis)} = 23$ Hz, 1H) ppm. ^{13}C NMR (101 MHz, CD_2Cl_2) δ ; 180.3 (C), 162.1 (C), 154.3 (C), 149.6 (C), 148.3 (C), 143.4 (2 x CH), 130.4 (CH), 128.7 (2 x CH), 128.6 (CH), 125.3 (CH), 119.6 (2 x CH), 70.3 (CH), 67.5 (CH₂), 57.8 (CH), 36.2 (d, $J_P = 43$ Hz, C), 30.6 (d, $J = 6$ Hz, CH), 28.6 (CH), 26.4 (3 x CH₃), 19.4 (CH₃), 18.3 (CH₃), 17.4 (CH₃), 16.2 (CH₃), 13.6 (CH₃), 9.1 (d, $J_P = 42$ Hz, CH₃) ppm. ^{31}P NMR (202 MHz, CDCl_3) δ ; 43.93 (d, $J_H = 19$ Hz) ppm. HRMS (nanoESI-Orbi) m/z : $[\text{M} - \text{Cl}]^+$ Calcd for $\text{C}_{29}\text{H}_{44}\text{IrN}_3\text{OP}$ 674.2846; Found 674.2835.

Supporting Information. Crystallographic data in CIF format file for **9** and **10**. NMR spectra for new compounds and HPLC chromatograms. This material is free of charge from the internet at <http://pubs.acs.org>.

Corresponding Authors

Email: xavier.verdaguer@irbbarcelona.org

Email: antoni.riera@irbbarcelona.org

Acknowledgments

We thank MINECO (CTQ2014-56361-P) and IRB Barcelona for financial support. E. S. thanks MINECO for a fellowship. IRB Barcelona is the recipient of a Severo Ochoa Award of Excellence from MINECO (Government of Spain).

References

- (1) *Asymmetric Catalysis on Industrial Scale*; Blaser, H.-U.; Schmidt, E., Eds.; Wiley-VCH: Weinheim, 2010.
- (2) a) Hopmann, K. H.; Bayer, A. Enantioselective Imine Hydrogenation with Iridium-Catalysts: Reactions, Mechanisms and Stereocontrol. *Coord. Chem. Rev.* **2014**, 268, 59–82. b) Fleury-Brégeot, N.; de la Fuente, V.; Castellón, S.; Claver, C. Highlights of Transition Metal-Catalyzed Asymmetric Hydrogenation of Imines. *ChemCatChem* **2010**, 2, 1346–1371. c) Xie, J.-H.; Zhu, S.-F.; Zhou, Q.-L. Transition Metal-Catalyzed Enantioselective Hydrogenation of Enamines and

Imines. *Chem. Rev.* **2011**, *111*, 1713–1760.

- (3) a) Baeza, A.; Pfaltz, A. Iridium-Catalyzed Asymmetric Hydrogenation of Imines. *Chem. Eur. J.* **2010**, *16*, 4003–4009. b) Moessner, C.; Bolm, C. Diphenylphosphanylsulfoximines as Ligands in Iridium-Catalyzed Asymmetric Imine Hydrogenations. *Angew. Chem. Int. Ed.* **2005**, *44*, 7564–7567. c) Trifonova, A.; Diesen, J. S.; Chapman, C. J.; Andersson, P. G. Application of Phosphine–Oxazoline Ligands in Ir-Catalyzed Asymmetric Hydrogenation of Acyclic Aromatic *N*-Arylimines. *Org. Lett.* **2004**, *6*, 3825–3827. and references cited therein.
- (4) a) Prades, A.; Núñez-Pertíñez, S.; Riera, A.; Verdaguer, X. P-Stereogenic Bisphosphines with a Hydrazine Backbone: From N–N Atropoisomerism to Double Nitrogen Inversion. *Chem. Commun.* **2017**, *53*, 4605–4608. b) Orgué, S.; Flores, A.; Biosca, M.; Pamies, O.; Diéguez, M.; Riera, A.; Verdaguer, X. Stereospecific SN2@P Reactions: Novel Access to Bulky P-Stereogenic Ligands. *Chem. Commun.* **2015**, *51*, 17548–17551.
- (5) Salomó, E.; Orgué, S.; Riera, A.; Verdaguer, X. Highly Enantioselective Iridium-Catalyzed Hydrogenation of Cyclic Enamides. *Angew. Chem. Int. Ed.* **2016**, *55*, 7988–7992.
- (6) Stankevič, M.; Andrijewski, G.; Pietrusiewicz, K. M. Direct Conversion of Sec - Phosphine Oxides into Phosphinous Acid-Boranes. *Synlett* **2004**, 0311–0315.
- (7) As determined by ¹H NMR spectroscopy, the acetophenone *N*-phenyl imine exists as a single *E* isomer, while 2-methoxyacetophenone *N*-phenyl imine and ethylphenylketone *N*-phenyl imine exist as a 70:30 and 92:8 mixture of *E/Z*

isomers respectively. In this scenario, each geometry of the imine substrate will be recognized by the catalyst differently and should provide different selectivity.

- (8) Pfaltz and coworkers stated that, for their catalytic system, BAr^F counter ion showed only a slight increase in reaction rate and no difference in enantiomeric excess with respect PF₆, see reference 3a.
- (9) Schramm, Y.; Barrios-Landeros, F.; Pfaltz, A. Discovery of an Iridacycle Catalyst with Improved Reactivity and Enantioselectivity in the Hydrogenation of Dialkyl Ketimines. *Chem. Sci.* **2013**, *4*, 2760-2766.
- (10) a) Hopmann, K. H.; Bayer, A. On the Mechanism of Iridium-Catalyzed Asymmetric Hydrogenation of Imines and Alkenes: A Theoretical Study. *Organometallics* **2011**, *30*, 2483–2497. b) Balcells, D.; Nova, A.; Clot, E.; Gnanamgari, D.; Crabtree, R. H.; Eisenstein, O. Mechanism of Homogeneous Iridium-Catalyzed Alkylation of Amines with Alcohols from a DFT Study. *Organometallics* **2008**, *27*, 2529–2535. c) Landaeta, V. R.; Muñoz, B. K.; Peruzzini, M.; Herrera, V.; Bianchini, C.; Sánchez-Delgado, R. A. Imine Hydrogenation by Tribenzylphosphine Rhodium and Iridium Complexes. *Organometallics* **2006**, *25*, 403–409. d) Martín, M.; Sola, E.; Tejero, S.; Andrés, J. L.; Oro, L. A. Mechanistic Investigations of Imine Hydrogenation Catalyzed by Cationic Iridium Complexes. *Chem. Eur. J.* **2006**, *12*, 4043–4056. e) Chen, H.-Y. T.; Wang, C.; Wu, X.; Jiang, X.; Catlow, C. R. A.; Xiao, J. Iridicycle-Catalysed Imine Reduction: An Experimental and Computational Study of the Mechanism. *Chem. Eur. J.* **2015**, *21*, 16564–16577.
- (11) Tutkowski, B.; Kerdphon, S.; Limé, E.; Helquist, P.; Andersson, P. G.; Wiest, O.; Norrby, P.-O. Revisiting the Stereodetermining Step in Enantioselective Iridium-

Catalyzed Imine Hydrogenation. *ACS Catal.* **2018**, 8, 615–623.

- (12) Complex **9** (derived from **1b**) affords 90% ee; while, complex **10** (derived from **3b**) affords 65% ee of the opposite configuration. Compounds **9** and **10** with *pseudo*-enantiomeric reacting site should, in principle, afford enantiomers of the product amine with the similar selectivity.
- (13) Liu, Y.; Du, H. Chiral Dienes as “Ligands” for Borane-Catalyzed Metal-Free Asymmetric Hydrogenation of Imines. *J. Am. Chem. Soc.* **2013**, 135, 6810-6813.
- (14) Bonsignore, M.; Benaglia, M.; L. Raimondi, L.; Orlandi, M.; Celentano, G. Enantioselective reduction of ketoimines promoted by easily available (*S*)-proline derivatives. *Beilstein J. Org. Chem.* **2013**, 9, 633.
- (15) Kutlescha, K.; Venkanna, G.T.; Kempe, R. The Potassium Hydride Mediated Trimerization of Imines. *Chem. Commun.* **2011**, 47, 4183-4185.
- (16) Schwob, T.; Kempe, R. A Reusable Co Catalyst for the Selective Hydrogenation of Functionalized Nitroarenes and the Direct Synthesis of Imines and Benzimidazoles from Nitroarenes and Aldehydes. *Angew. Chem. Int. Ed.* **2016**, 55, 15175-15179.
- (17) Kumaran, E.; Leong, W. K. Rhodium(III)-Catalyzed Hydroamination of Aromatic Terminal Alkynes with Anilines. *Organometallics* **2012**, 31 (3), 1068–1072.
- (18) Wang, G.; Chen, C.; Du, T.; Zhong, W. Metal-free Catalytic Hydrogenation of Imines with Recyclable [2.2]paracyclophane-derived Frustrated Lewis Pairs Catalysts. *Adv. Synth. Catal.* **2014**, 356, 1747.
- (19) Wübbolt, S.; Maji, M. S.; Irran, E.; Oestreich, M. A Tethered Ru–S Complex with

- an Axial Chiral Thiolate Ligand for Cooperative Si–H Bond Activation: Application to Enantioselective Imine Reduction. *Chem. Eur. J.* **2017**, *23*, 6213-6219.
- (20) Sun, Q.; Wang, Y.; Yuan, D.; Yao, Y.; Shen, Q. Synthesis of Group 4 Metal Complexes Stabilized by an Amine-Bridged Bis(phenolato) Ligand and Their Catalytic Behavior in Intermolecular Hydroamination Reactions. *Organometallics* **2014**, *33*, 994-1001.